

Effect of α - Q value on incomplete fusion

Abhishek Yadav,^{1,*} Vijay R. Sharma,¹ Pushpendra P. Singh,^{2,†} R. Kumar,³ D. P. Singh,¹ Unnati,¹ M. K. Sharma,⁴ B. P. Singh,^{1,‡} and R. Prasad¹

¹*Department of Physics, A.M. University, Aligarh (UP) - 202 002, India*

²*GSI Helmholtz Centre for Heavy Ion Research GmbH, D-64291 Darmstadt, Germany*

³*NP-Group, Inter-University Accelerator Centre, New Delhi-110067, India*

⁴*Physics Department, S.V. College, Aligarh (UP) - 202 002, India*

(Received 4 May 2012; published 5 July 2012)

The probability of incomplete fusion in $^{13}\text{C} + ^{159}\text{Tb}$ interactions has been measured in the energy range $\approx 4\text{--}7$ MeV/nucleon. The variation of the incomplete fusion fraction has been studied in terms of projectile energy and type. Present results are compared with the existing $^{12}\text{C} + ^{159}\text{Tb}$ data, where a strong projectile structure effect on the incomplete fusion fraction has been observed. It has been found that the probability of incomplete fusion is higher in the case of ^{12}C than for a one-neutron rich ^{13}C projectile. For better insight into the projectile structure effect, a systematic study is presented on the incomplete fusion measured in $^{12,13}\text{C}, ^{16}\text{O} + ^{159}\text{Tb}$ and $^{12,13}\text{C}, ^{16}\text{O} + ^{181}\text{Ta}$ systems by Singh *et al.* [*Phys. Rev. C* **80**, 014601 (2009)] and by Babu *et al.* [*J. Phys. G* **29**, 1011 (2003)]. The present analysis indicates a strong dependence of incomplete fusion probability on the α - Q value of the projectile at these low energies.

DOI: [10.1103/PhysRevC.86.014603](https://doi.org/10.1103/PhysRevC.86.014603)

PACS number(s): 25.60.Dz, 25.70.Gh, 25.70.Jj, 25.70.Mn

I. INTRODUCTION

Much interest has been shown in recent years in the study of incomplete fusion (ICF) reaction dynamics in heavy-ion interactions at low incident energies, i.e., from slightly above barrier energies to well above them [1–10]. The observation of ICF events in heavy-ion (HI) induced reactions dates back to the 1970s, when Britt and Quinton first observed the fast α particles in massive transfer reactions at $E_{\text{lab}} \geq 10.5$ MeV/nucleon [11]. Since then ICF has been extensively investigated and established as one of the competing modes of reaction at $E_{\text{lab}} \approx 7\text{--}10$ MeV/nucleon [2,8–10,12–17]. Although, complete fusion (CF) has been considered to be the sole contributor to the total fusion cross section at these energies [18,19], recent studies demonstrate substantial ICF contributions at energies < 10 MeV/nucleon [2–4,8–10].

A variety of theoretical models have been proposed to understand ICF reaction dynamics [1,12–14,20–22]. The most widely used and accepted descriptions of ICF are based on the breakup fusion (BUF) [13] and sum-rule models [21,22]. According to the BUF model, CF and ICF events can be disentangled on the basis of the degree of linear momentum transfer (LMT) from the projectile to the target nucleus. In the case of CF, entire nucleonic degrees of freedom of projectile and target nucleus blend to form an equilibrated compound nucleus (CN) with predetermined physical properties, e.g., charge, mass, recoil velocity, etc. However, the ICF events originate from the fractional LMT followed by projectile breakup. It may be pointed out that the additional breakup

degrees of freedom may give rise to several reaction processes, such as (a) the noncapture breakup (NCBU), when none of the breakup fragments are captured, (b) sequential complete fusion (SCF), the successive capture of all the projectile fragments by the target nucleus, and (c) incomplete fusion (ICF), when one of the breakup fragments is captured. Experimentally, it is not possible to distinguish normal and sequential CF events because of the identical residues in the exit channel. On the other hand, the sum-rule model takes driven input angular momenta (ℓ values) into account to describe CF and ICF processes. The ℓ values from $\ell = 0$ to ℓ_{crit} lead to the CF events; however, for $\ell \geq \ell_{\text{crit}}$, ICF events are expected to set in. In the latter case, (for ℓ values higher than ℓ_{crit}) the absence of potential pocket forbids fusion until a part of the projectile is released (P^s : spectator) to provide sustainable input angular momenta [21–23]. After such an emission, the remnant (P^p : participant) is supposed to carry input angular momenta less and/or equal to its own critical limit ($\ell_{\text{eff}} \leq \ell_{\text{crit}}^{P^p+T}$) for fusion to occur.

The LMTs in CF and/or ICF events obtained from the analysis of recoil-momentum distributions measured at different energies have been explained fairly well by the BUF model, and suggest the onset of ICF even at slightly above barrier energies [10]. Other existing models and theories explain the ICF data obtained at energies ≥ 7 MeV/nucleon to some extent, but completely fail at lower energies [12,14,20]. Contrary to the experimental observations, the sum-rule model predicts negligibly small ICF cross sections at $\approx 4\text{--}7$ MeV/nucleon [10,24]. Existence of ICF at low incident energies and/or below the values of ℓ_{crit} (for CF) has been claimed by different groups [25–27]. In addition to this, the unclear or ambiguous dependences of ICF on various entrance channel parameters, viz., projectile type and energy, driving angular momentum (ℓ) into the system, binding energy and/or α - Q value (Q_α), mass asymmetry [$\mu_A = A_T/(A_T + A_P)$], deformation of interacting partners, etc., are also required to

* abhishekyadav117@gmail.com

† pushpendrasingh@gmail.com; Also at the Institute for Nuclear Physics, Technical University Darmstadt, D-64289 Darmstadt, Germany.

‡ bpsinghamu@gmail.com

be explored. Several contradicting dependences of the fraction of incomplete fusion (F_{ICF}), which is a measure of relative strength of ICF to the total fusion, have been discussed in recent reports [3,4,24–30]. In Refs. [4,25] it has been found that the F_{ICF} is independent of the target charge (Z_T) and thus from $Z_P Z_T$. However, in Ref. [26] of the same group the fusion suppression is predicted to be almost proportional to the charge Z_T of target nucleus. In a recent paper by Gomes *et al.* [27] a trend of systematic behavior for the F_{ICF} as a function of the Z_T is discussed. Morgenstern *et al.* [28] correlated the ICF fraction with entrance channel mass asymmetry (μ_A). Recently, Singh *et al.* [29] supplemented Morgenstern's mass-asymmetry systematics by introducing the importance of projectile structure. Apart from this, one of our recent works [30] reported the dependence of F_{ICF} on the target mass or $Z_P Z_T$ of interacting partners for a wide range of projectile-target combinations. Furthermore, Geoffroy *et al.* [15] suggested the origin of ICF events from undamped noncentral interactions. The noncentral nature of ICF events has also been emphasized by Trautmann *et al.* [16], Inamura *et al.* [17], and Zolonowski *et al.* [31]. In a outstanding review, Gerschel [32] presented several dependences of ICF. In the case of rare-earth targets, the ICF has been found to be originated from relatively high ℓ values [33], but the results obtained by Tricoire *et al.* [34] with semimagic targets suggest the contribution of ICF events from ℓ values even smaller than $0.5\ell_{crit}$ [35,36]. Almost similar conclusions have been drawn by Tserruya *et al.* [37] and Oeschler *et al.* [38], who observed both CF and ICF below and above the value of ℓ_{crit} .

The ambiguous dependence of ICF on various entrance channel parameters needs serious attention. To investigate ICF reaction dynamics in detail, we have undertaken a program to study ICF fractions in terms of various entrance channel observables. In this work, the ICF fraction (F_{ICF}) has been deduced from the analysis of experimental excitation functions (EFs) of individual reaction residues produced in the $^{13}\text{C} + ^{159}\text{Tb}$ system at energies $\approx 4\text{--}7$ MeV/nucleon. The present results are compared with the existing $^{12}\text{C} + ^{159}\text{Tb}$ data [30]. This reveals the first sign of an α - Q value effect on the ICF fraction.

II. EXPERIMENTS

The experiments were performed using the 15UD-Pelletron accelerator of the Inter-University Accelerator Center (IUAC), New Delhi, India, employing an activation technique. The experimental setup and procedures are the same as in Ref. [30]. Here, a short account of experimental conditions are given, and we refer the reader to the recent paper [30] for further details. Natural ^{159}Tb targets of thickness ≈ 1.2 mg/cm² and Al foils of thicknesses $\approx 1.5\text{--}2.5$ mg/cm² were prepared by a rolling technique. Each target was backed by an Al foil of appropriate thickness (hereafter called the target-catcher foil assembly) to stop heavy recoiling products produced in the reactions. To cover a wide energy range in the limited beam time, a stacked-foil energy degradation procedure was used. Five stacks, with three target-catcher foil assemblies in each, were bombarded by a ^{13}C beam at energies E_{lab}

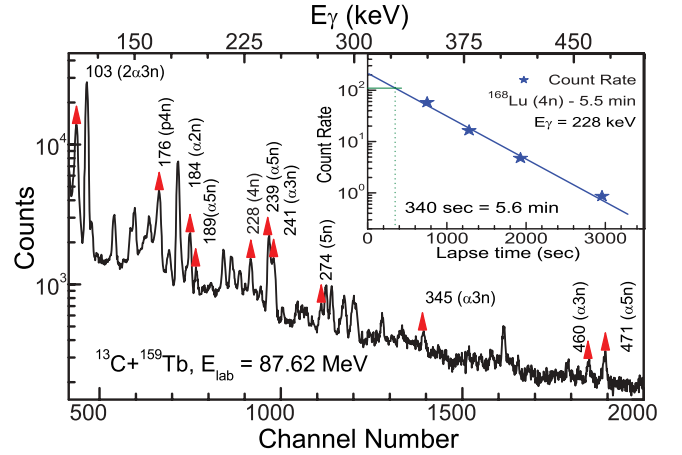


FIG. 1. (Color online) Typical γ -ray spectrum obtained at 87.62 ± 0.38 MeV in $^{13}\text{C} + ^{159}\text{Tb}$ interactions. Some of the identified γ lines corresponding to different CF and/or ICF residues are labeled.

$\approx 58, 60, 70, 73, 85,$ and 88 MeV with beam intensities $\approx 3\text{--}4$ pnA. The target-catcher foil assemblies were taken out from the scattering chamber for off-line activity measurements. The activities produced in the individual target-catcher foil assemblies were counted with a precalibrated HPGGe detector coupled to an in-line CAMAC data-acquisition system [39]. The HPGGe detector was calibrated for energy and efficiency using standard γ sources of known strength. The evaporation residues were identified by their characteristic γ lines, and verified by their decay-curve analysis. Figure 1 shows a part of the γ spectra and the decay curve of ^{168}Lu ($t_{1/2} = 5.5$ min) residues (inset of Fig. 1) populated via $^{13}\text{C} + ^{159}\text{Tb}$ interactions at $E_{lab} \approx 87.6 \pm 0.38$ MeV. Some of the γ lines are marked with the corresponding evaporation residues. The energy-dependent production cross section of evaporation residues (σ_{ER}) have been determined [24]. The overall error in the measured σ_{ER} is estimated to be $\leq 15\%$. A detailed discussion on error analysis is given elsewhere [30].

The excitation functions (EFs) of residues $^{169,168,167}\text{Lu}$ ($xn; x = 3\text{--}5$), ^{167}Yb ($p4n$), $^{166,165,163}\text{Tm}$ ($\alpha xn; x = 2, 3, 5$) and $^{162,161,160}\text{Ho}$ ($2 \alpha xn; x = 2\text{--}4$) produced in $^{13}\text{C} + ^{159}\text{Tb}$ interactions in the energy range $\approx 1.01V_b$ to $1.68V_b$ ($V_b \approx 52$ MeV) have been measured and are analyzed within the framework of the statistical model code PACE4 [40]. Detailed definition and listing of input parameters of this code are presented elsewhere [29,30,40–42]. The code PACE4 takes formation and decay of CF events into account according to the Hauser-Feshbach theory of CN decay, therefore, any deviation in the experimental EFs from the PACE4 calculations may be attributed to the onset of ICF. In this code, the level density parameter ($a = A/K$) is an important input parameter which may be varied to reproduce the experimental EFs.

A. Analysis and interpretation of results

The experimentally measured and theoretically calculated EFs of all $xn + pxn$ channels ($\Sigma \sigma_{xn+pxn}$, i.e., the sum of the cross sections of $^{169,168,167}\text{Lu}$ and ^{167}Yb residues) are

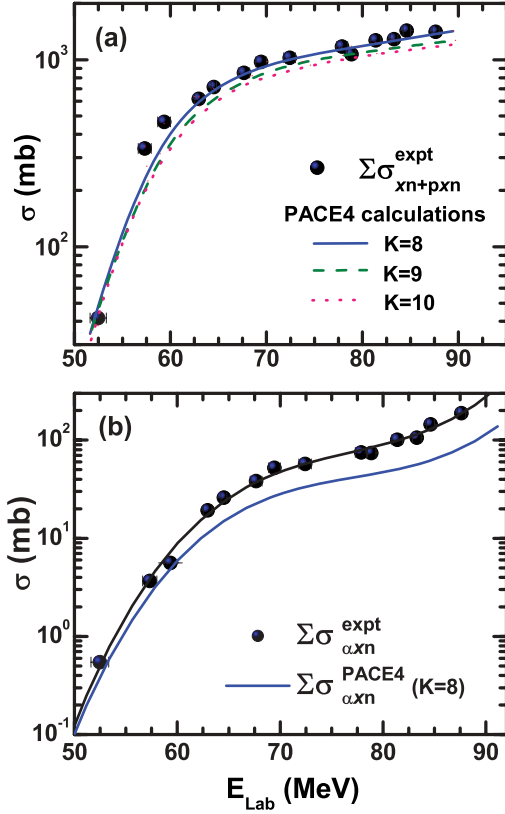


FIG. 2. (Color online) (a) Sum of cross sections for xn and pxn channels to calibrate the parameters of PACE4 code for the $^{13}\text{C} + ^{159}\text{Tb}$ system, which shows production of these channels via the CF process. (b) Comparison of cross section of α -emitting channels with PACE4 code, which shows enhancement over theoretical predictions with same set of parameters as used to reproduce xn and pxn channels (for details see the text).

compared in Fig. 2(a) with corresponding PACE4 calculations. It is not out of place to mention that the evaporation residue ^{167}Yb ($p4n$) is found to be strongly fed from its higher charge isobar (precursor hereafter) ^{167}Lu ($5n$) through β^+ emission. As such, the independent production cross section of $^{167}\text{Yb}^{\text{ind}}$ has been deduced using the prescription given in Ref. [43]. Lines and symbols are self-explanatory. As can be seen from this figure, the PACE4 calculations reproduce, fairly well, the experimental data with a value of level density parameter $a = A/8 \text{ MeV}^{-1}$. This confirms the population of $^{169,168,167}\text{Lu}$ (xn ; $x = 3-5$), and ^{167}Yb ($p4n$) residues via CF of ^{13}C with ^{159}Tb . As such, the value of $a = A/8 \text{ MeV}^{-1}$ can be used as the default parameter for further analysis. To figure out if the α -emitting channels are populated via CF, the experimental EFs of all α -emitting channels ($\Sigma\sigma_{\alpha xn+2\alpha xn}$, i.e., the sum of the cross sections of $^{166,165,163}\text{Tm}$ and $^{162,161,160}\text{Ho}$ residues) are compared with the predictions of PACE4 in Fig. 2(b). The calculations are performed using the same set of input parameters used to reproduce the xn and pxn channels. As can be seen from Fig. 2(b), the experimental EFs are significantly enhanced as compared to the PACE4 predictions, which points towards the observation of ICF contributions at these energies.

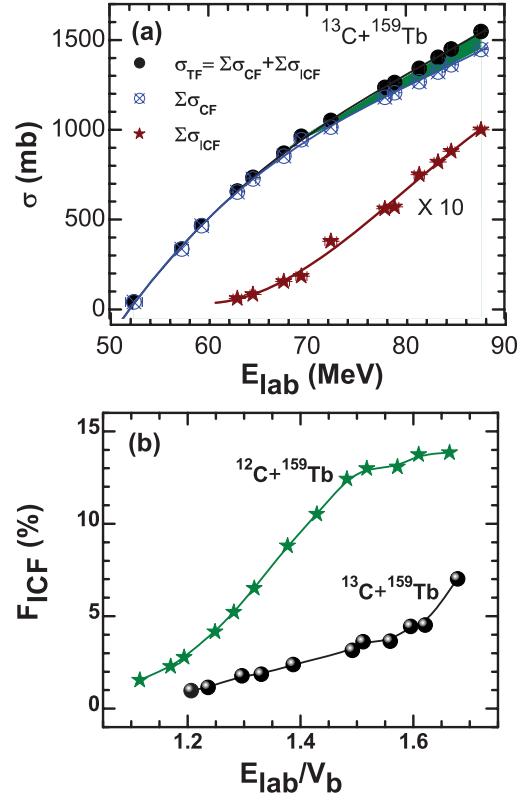


FIG. 3. (Color online) (a) Comparison of total, complete, and incomplete fusion cross sections for $^{13}\text{C} + ^{159}\text{Tb}$ system. (b) Comparison of F_{ICF} for $^{12}\text{C} + ^{159}\text{Tb}$ and $^{13}\text{C} + ^{159}\text{Tb}$ systems (for details see the text).

The $^{166,165,163}\text{Tm}$ and $^{162,161,160}\text{Ho}$ residues are likely to be populated via CF and/or ICF in the following ways:

- (i) CF: the projectile ^{13}C completely fuses with the target nucleus ^{159}Tb to form an excited system $^{172}\text{Lu}^*$, which eventually decays via light nuclear particles and/or one or two α clusters together with the neutrons and/or protons to produce Tm and Ho isotopes.
- (ii) ICF: the projectile may break up into its constituent α clusters (i.e., $^{13}\text{C} \rightarrow ^8\text{Be} + ^4\text{He} + n$). One of the fragments fuses with the target nucleus to form a reduced CN, and the remnant behaves as a spectator. The reduced CN may also decay via neutron and/or proton emission to reach the aforementioned isotopes.

As shown in Fig. 2(b), the enhancement in the production cross sections for α -emitting channels over the PACE4 calculations increases with the incident energy, which directly correlates the incident energy and ICF fraction. To reconfirm this aspect, the data presented in Fig. 2 have been analyzed using a well-established data reduction procedure [29,30]. The fraction of ICF in α -emitting channels has been accounted as $\Sigma\sigma_{\text{ICF}} = \Sigma\sigma_{\alpha xn}^{\text{expt}} - \Sigma\sigma_{\alpha xn}^{\text{theor}}$, and is plotted as a function of energy in Fig. 3(a). The lines and curves are the outcome of best-fitting procedure. To show how the ICF contributes to the total fusion cross section, the sum of all CF channels ($\Sigma\sigma_{\text{CF}}$) is also plotted in Fig. 3(a) along with total fusion (i.e.,

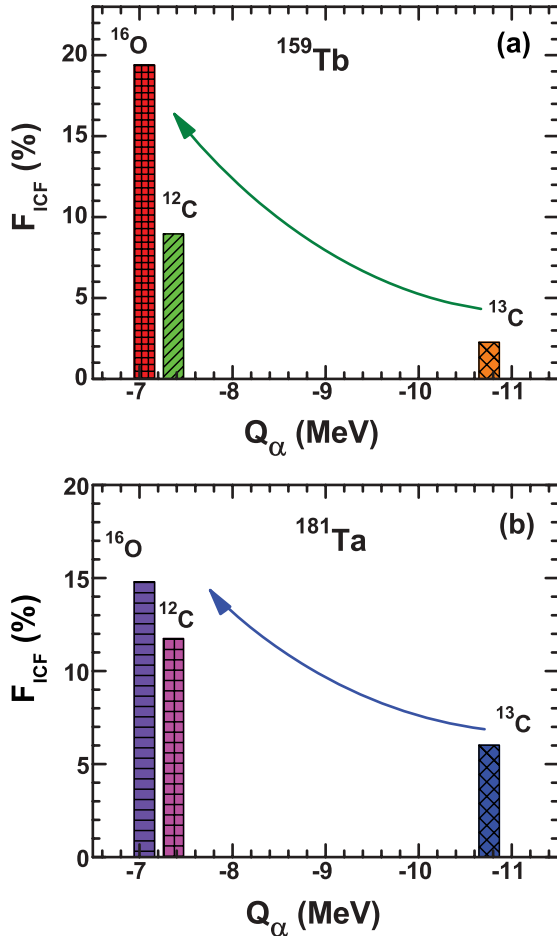


FIG. 4. (Color online) Comparison of F_{ICF} on the basis of Q_α value at a constant $v_{rel} = 0.053$ (for details see the text).

$\sigma_{TF} = \Sigma\sigma_{CF} + \Sigma\sigma_{ICF}$) as a function a energy. The onset of ICF is clearly evident at energies as low as ≈ 63 MeV (i.e., 21% above the barrier) and increases almost linearly for higher energies.

For better insight into the onset and influence of ICF in terms of various entrance channel parameters, the percentage fraction of ICF (F_{ICF}) has been deduced from the analysis of data presented in Fig. 3(a). The F_{ICF} is a measure of the relative strength of ICF to the total fusion, defined as $F_{ICF}(\%) = (\Sigma\sigma_{ICF}/\sigma_{TF}) \times 100$. The mapping of ICF strength with incident energy is termed the ICF strength function [29]. To figure out how the projectile structure affects the ICF strength, the ICF strength functions for $^{13}\text{C} + ^{159}\text{Tb}$ and $^{12}\text{C} + ^{159}\text{Tb}$ (from Ref. [30]) systems are plotted in Fig. 3(b). The energy axis is normalized to correct for the different Coulomb barriers of the two systems. As shown in this figure, the probability of ICF ($\%F_{ICF}$) for the ^{13}C projectile is noticeably smaller than that for the ^{12}C projectile in the entire energy range. In case of ^{12}C , the onset of ICF is at a relatively lower energy (i.e., $1.1V_b$) than for ^{13}C induced reactions. The strikingly different ICF fractions for ^{13}C and ^{12}C induced reactions point mainly towards the projectile structure effect. It may be pointed out that ^{12}C is a well-known α -cluster nucleus with $Q_\alpha \approx -7.37$ MeV.

However, ^{13}C has a larger Q_α value (≈ -10.64 MeV) than ^{12}C . The higher Q_α value for ^{13}C translates into the smaller breakup probability into constituent α clusters, resulting in a smaller ICF fraction than for ^{12}C induced reactions [44].

To validate the above-mentioned Q_α -value systematics, the probability of ICF ($\%F_{ICF}$) has been deduced for ^{12}C , ^{13}C , and ^{16}O induced reactions on the two sets of targets ^{159}Tb [29,30] and ^{181}Ta [45,46] at a constant relative velocity $v_{rel} = 0.053$ [29,30,45,46], and plotted with Q_α values in Fig. 4. The values of F_{ICF} for all six projectile-target combinations are found to follow the same trend as observed for $^{12}\text{C}, ^{13}\text{C} + ^{159}\text{Tb}$ systems presented in Fig. 3(b). The probability of ICF is found to be less for larger Q_α -value projectiles. For example, the value of F_{ICF} for the ^{16}O ($Q_\alpha \approx -7.16$ MeV) + ^{159}Tb system [29] is found to be $\approx 19\%$ which is reduced to only $\approx 3\%$ for the ^{13}C ($Q_\alpha \approx -10.64$ MeV) + ^{159}Tb system [46]. The same systematics was followed for the ^{181}Ta target. Hence, from the data presented in Fig. 4, it can be inferred that the Q_α value is an important entrance channel parameter which essentially dictates the probability of ICF.

Further, as shown in Fig. 4, the value of F_{ICF} is found to be $\approx 3\%$ and $\approx 7\%$ for $^{13}\text{C} + ^{159}\text{Tb}$ and $^{13}\text{C} + ^{181}\text{Ta}$, $\approx 9\%$ and $\approx 11\%$ for $^{12}\text{C} + ^{159}\text{Tb}$ and $^{12}\text{C} + ^{181}\text{Ta}$, and $\approx 19\%$ and $\approx 15\%$ for $^{16}\text{O} + ^{159}\text{Tb}$ and $^{16}\text{O} + ^{181}\text{Ta}$, respectively. The value of F_{ICF} for $^{16}\text{O} + ^{181}\text{Ta}$ is expected to go up; as indicated in Ref. [45], all the α channels could not be measured for this system. The value of F_{ICF} for the given projectile-target combinations supports Morgenstern's mass-asymmetry systematics [28] along with the projectile structure supplement given by Singh *et al.* [29].

III. CONCLUSION

In summary, the probability of low energy ICF has been measured in the $^{13}\text{C} + ^{159}\text{Tb}$ system from the analysis of differential EFs within the framework of statistical model code PACE4. To the best of our knowledge, the first sign of an α - Q -value effect on the ICF fraction has been observed for strongly bound projectiles. The fraction of ICF has been found to decrease for projectiles having large negative α - Q values. If confirmed for other projectile-target combinations, this may provide an important input to understanding the complex ICF dynamics at low incident energies. More experiments are planned to cover this aspect thoroughly.

ACKNOWLEDGMENTS

The authors thank the Pelletron technical staff for providing excellent ^{13}C beams, and Prof. A. Roy for extending experimental facilities to perform this experiment. We sincerely acknowledge several scientific discussions with Prof. R. K. Bhowmik, and the help recieved from Dr. S. Muralithar and Dr. R. P. Singh during the experiments. A.Y. thanks the University Grant Commission (UGC) of the Government of India for the SRF grant. B.P.S. and R.P. thank the UGC for financial support.

- [1] A. Diaz-Torres, D. J. Hinde, J. A. Tostevin, M. Dasgupta, and L. R. Gasques, *Phys. Rev. Lett.* **98**, 152701 (2007); A. Diaz-Torres and I. J. Thompson, *Phys. Rev. C* **65**, 024606 (2002).
- [2] F. K. Amanuel *et al.*, *Phys. Rev. C* **84**, 024614 (2011).
- [3] P. R. S. Gomes *et al.*, *Phys. Rev. C* **84**, 014615 (2011).
- [4] R. Rafiei *et al.*, *Phys. Rev. C* **81**, 024601 (2010).
- [5] H. Esbensen, *Phys. Rev. C* **81**, 034606 (2010).
- [6] M. Dasgupta, D. J. Hinde, A. Mukherjee, and J. O. Newton, *Nucl. Phys. A* **787**, 144 (2007).
- [7] M. Dasgupta *et al.*, *Phys. Rev. C* **66**, 041602(R) (2002).
- [8] Pushpendra P. Singh *et al.*, *Phys. Lett. B* **671**, 20 (2009), and references therein.
- [9] Pushpendra P. Singh *et al.*, *J. Phys.: Conf. Ser.* **282**, 012019 (2011).
- [10] Devendra P. Singh *et al.*, *Phys. Rev. C* **81**, 054607 (2010).
- [11] H. C. Britt and A. R. Quinon, *Phys. Rev.* **124**, 877 (1961).
- [12] J. P. Bondroff *et al.*, *Nucl. Phys. A* **333**, 285 (1980).
- [13] T. Udagawa and T. Tamura, *Phys. Rev. Lett.* **45**, 1311 (1980).
- [14] J. R. Wu and I. Y. Lee, *Phys. Rev. Lett.* **45**, 8 (1980).
- [15] K. A. Geoffroy *et al.*, *Phys. Rev. Lett.* **43**, 1303 (1979).
- [16] W. Trautmann *et al.*, *Phys. Rev. Lett.* **53**, 1630 (1984).
- [17] T. Inamura, T. Kojima, T. Nomura, T. Sugitate and H. Utsunomiya, *Phys. Lett. B* **84**, 71 (1979); *Phys. Rev. C* **32**, 1539 (1985); *Phys. Lett. B* **68**, 51 (1977).
- [18] H. H. Gutbrod *et al.*, *Nucl. Phys. A* **213**, 267 (1973).
- [19] P. David *et al.*, *Nucl. Phys. A* **287**, 179 (1977).
- [20] R. Weiner and Westrom, *Nucl. Phys. A* **386**, 282 (1977).
- [21] J. Wilczynski *et al.*, *Nucl. Phys. A* **373**, 109 (1982); *Phys. Rev. Lett.* **45**, 606 (1980).
- [22] K. Siwek-Wilczynska *et al.*, *Phys. Rev. Lett.* **42**, 1599 (1979).
- [23] P. E. Hodgson, E. Gadioli, and E. Gadioli Erba, *Introductory Nuclear Physics* (Clarendon, Oxford, 1997).
- [24] Unnati Gupta *et al.*, *Nucl. Phys. A* **811**, 77 (2008); *Phys. Rev. C* **80**, 024613 (2009).
- [25] L. R. Gasques *et al.*, *Phys. Rev. C* **79**, 034605 (2009).
- [26] D. J. Hinde, M. Dasgupta, B. R. Fulton, C. R. Morton, R. J. Wooliscroft, A. C. Berriman, and K. Hagino, *Phys. Rev. Lett.* **89**, 272701 (2002).
- [27] P. R. S. Gomes *et al.*, *Phys. Rev. C* **73**, 064606 (2006); *Phys. Lett. B* **601**, 20 (2004).
- [28] H. M. Morgenstern *et al.*, *Phys. Rev. Lett.* **52**, 1104 (1984); *Z. Phys. A* **313**, 39 (1983); *Phys. Lett. B* **113**, 463 (1982).
- [29] Pushpendra P. Singh *et al.*, *Phys. Rev. C* **77**, 014607 (2008); *Euro. Phys. J. A* **34**, 29 (2007).
- [30] Abhishek Yadav *et al.*, *Phys. Rev. C* **85**, 034614 (2012).
- [31] D. R. Zolnowski *et al.*, *Phys. Lett.* **41**, 92 (1978).
- [32] C. Gerschel, *Nucl. Phys. A* **387**, 297 (1982).
- [33] J. H. Barker *et al.*, *Phys. Rev. Lett.* **45**, 424 (1980).
- [34] H. Tricoire, C. Gerschel, A. Gillibert, and N. Perrin, *Z. Phys. A-Atomic Nuclei* **323**, 163 (1986).
- [35] R. L. Robinson *et al.*, *Phys. Rev. C* **24**, 2084 (1981).
- [36] H. Utsunomiya *et al.*, *Phys. Lett. B* **105**, 135 (1981).
- [37] I. Tserruya *et al.*, *Phys. Rev. Lett.* **60**, 14 (1988).
- [38] H. Oeschler *et al.*, *Phys. Lett. B* **127**, 177 (1983).
- [39] CANDLE-Collection and Analysis of Nuclear Data using Linux network, B. P. Ajith Kumar *et al.* DAE SNP, 2001, Kolkotta.
- [40] A. Gavron, *Phys. Rev. C* **21**, 230 (1980).
- [41] S. K. Kataria, V. S. Ramamurthy, and S. S. Kapoor, *Phys. Rev. C* **18**, 549 (1978).
- [42] R. Bass, *Nucl. Phys. A* **231**, 45 (1974).
- [43] Robley D. Evans, *The Atomic Nucleus* (McGraw-Hill, New York, 1955).
- [44] Abhishek Yadav *et al.*, *EPJ Web Conf.* **21**, 08005 (2012).
- [45] Devendra P. Singh *et al.*, *Phys. Rev. C* **80**, 014601 (2009).
- [46] K. Sudarsan Babu *et al.*, *J. Phys. G* **29**, 1011 (2003).